



# Synthesis of deuterated $\gamma$ -linolenic acid and application for biological studies: metabolic tuning and Raman imaging†

Cite this: *Chem. Commun.*, 2021, **57**, 2180

Received 1st December 2020,  
Accepted 26th January 2021

DOI: 10.1039/d0cc07824g

rsc.li/chemcomm

Kosuke Dodo,<sup>ib</sup>\*<sup>abcd</sup> Ayato Sato,<sup>ib</sup><sup>ab</sup> Yuki Tamura,<sup>ib</sup><sup>ab</sup> Syusuke Egoshi,<sup>ac</sup>  
Koichi Fujiwara,<sup>ac</sup> Kana Oonuma,<sup>d</sup> Shuhei Nakao,<sup>ib</sup><sup>ac</sup> Naoki Terayama,<sup>ib</sup><sup>acd</sup> and  
Mikiko Sodeoka,<sup>ib</sup>\*<sup>abcd</sup>

$\gamma$ -Linolenic acid (GLA) is reported to show tumor-selective cytotoxicity through unidentified mechanisms. Here, to assess the involvement of oxidized metabolites of GLA, we synthesized several deuterated GLAs and evaluated their metabolism and cytotoxicity towards normal human fibroblast WI-38 cells and VA-13 tumor cells generated from WI-38 by transformation with SV40 virus. Deuteration of GLA suppressed both metabolism and cytotoxicity towards WI-38 cells and increased the selectivity for VA-13 cells. Fully deuterated GLA was visualized by Raman imaging, which indicated that GLA is accumulated in intracellular lipid droplets of VA-13 cells. Our results suggest the tumor-selective cytotoxicity is due to GLA itself, not its oxidized metabolites.

Polyunsaturated fatty acids (PUFAs) are transformed into metabolites that regulate various biological phenomena. Among them, arachidonic acid (AA) is a precursor of various eicosanoids, including prostaglandins and leukotrienes, which are both physiologically and pathologically important.<sup>1</sup> Initial transformation of AA is mainly mediated by oxidizing enzymes, such as cyclooxygenase (COX) and lipoxygenase (LOX). Non-enzymatic auto-oxidation reactions of AA also produce bioactive metabolites *via* the generation of lipid radicals.<sup>2</sup> Other PUFAs such as eicosapentaenoic acid (EPA) and docosahexaenoic acid (DHA) also afford bioactive metabolites.<sup>3</sup> Therefore, it is possible that unidentified metabolites derived from PUFAs are biologically active.

Among the PUFAs,  $\gamma$ -linolenic acid (GLA) was reported to show anticancer activity *via* an unidentified mechanism.<sup>4</sup> In contrast to its cytotoxic effects towards various tumor cell lines, GLA was much less toxic to normal cells, and free radicals generated from GLA were proposed to mediate the cytotoxicity in a cell-line-specific manner.<sup>5–7</sup> However, the details remain unclear.

Recent studies indicate that deuteration of the bis-allylic methylene structure suppresses both enzymatic and non-enzymatic metabolism of PUFAs.<sup>8–11</sup> In metabolic reactions of PUFAs, the abstraction of a hydrogen atom from the bis-allylic methylene is a critical step, producing a delocalized radical. The kinetic isotope effect (KIE) of deuterium inhibits this abstraction step, and thus inhibits the subsequent metabolism of PUFAs. In this work, we planned to examine the effect of metabolic inhibition of GLA on the cytotoxicity by introducing deuterium into the bis-allylic positions (Fig. 1). Evaluation of deuterated sites that affect the activity of GLA could help to identify the key reaction sites for generating putative cytotoxic metabolites.

In addition, deuterium serves as a tag for Raman imaging.<sup>12</sup> Tumor-selective effects of GLA might be due to differences in the cellular uptake or distribution of GLA. Therefore, we aimed to examine this possibility by employing Raman imaging. The

<sup>a</sup> Synthetic Organic Chemistry Laboratory, RIKEN Cluster for Pioneering Research, 2-1 Hirosawa, Wako, Saitama 351-0198, Japan. E-mail: sodeoka@riken.jp, dodo@riken.jp

<sup>b</sup> Sodeoka Live Cell Chemistry Project, ERATO, Japan Sciences and Technology Agency, 2-1 Hirosawa, Wako, Saitama 351-0198, Japan

<sup>c</sup> AMED-CREST, Japan Agency for Medical Research and Development, 2-1 Hirosawa, Wako, Saitama 351-0198, Japan

<sup>d</sup> RIKEN Center for Sustainable Resource Science, 2-1 Hirosawa, Wako, Saitama 351-0198, Japan

† Electronic supplementary information (ESI) available: Experimental procedures, supplemental data, and spectral data. See DOI: 10.1039/d0cc07824g

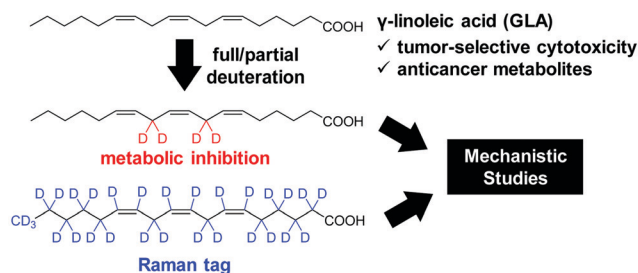


Fig. 1 Applications of deuterated  $\gamma$ -linolenic acid (GLA) derivatives for mechanistic studies.

C–D bond has a specific Raman peak in the silent region where cellular endogenous molecules have no Raman signal. Although the Raman signal of C–D is very weak compared with that of an alkyne moiety, which was previously developed as a Raman tag for live-cell imaging,<sup>13–16</sup> highly deuterated fatty acids have been used as probes for live-cell Raman imaging.<sup>17,18</sup> Therefore, we planned to apply deuterated GLA for live-cell Raman imaging (Fig. 1).

We firstly introduced deuterium at the bis-allylic methylenes, C-8 and/or C-11, in order to examine the effects on metabolism. As shown in Scheme 1, deuterated methylene unit **2** was synthesized from TMS-acetylene **1**. Lithium acetylide derived from **1** was reacted with deuterated paraformaldehyde, and then protection of the alcohol with THP and deprotection of a TMS group afforded **2**. In the same manner, normal or deuterated paraformaldehyde was reacted with lithium acetylide generated from 1-heptyne **3**, and the alcohol group was tosylated<sup>19</sup> to afford **4a** or **4b** having the C-11 methylene group of GLA. The C-8 methylene group was then introduced by nucleophilic substitution of the OTs group with copper acetylide.<sup>20,21</sup> Compound **4a** was reacted with **2**, and then deprotection of the THP group followed by tosylation afforded **5a**. Compound **4b** was reacted with propargyl alcohol, and tosylation afforded **5b**. Compound **5c** was obtained from **4b** and **2** according to the same procedure used for **5a**. Compounds **5a–5c** were reacted with cuprate derived from methyl 6-heptynoate and successive hydrogenation with Ni(OAc)<sub>2</sub>–NaBH<sub>4</sub> afforded compounds **6a–6c**.<sup>22</sup> Finally, hydrolysis of the methyl ester gave the deuterated GLA derivatives **7a–7c**.

To evaluate the tumor-selective cytotoxicity of GLA, we used two cell lines, WI-38 and VA-13. WI-38 cells are normal human lung fibroblast cells, while VA-13 cells are tumor cells generated from WI-38 by transformation with SV40 virus. Therefore, the genetic background of the two cell lines is the same. First, WI-38 and VA-13 cells were treated with GLA for 48 h, and cell viability was determined by means of alamarBlue assay. As shown in Fig. 2, GLA showed stronger cytotoxicity towards

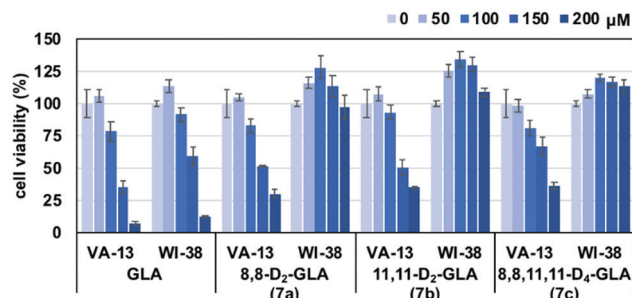
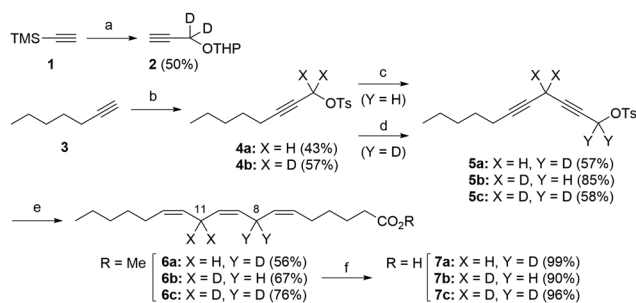


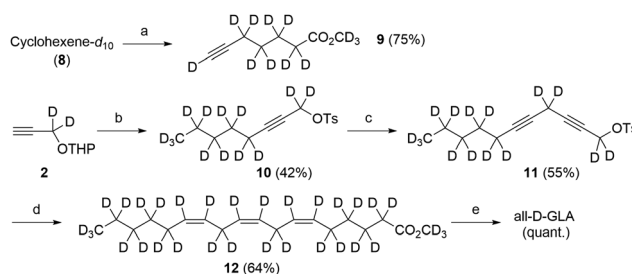
Fig. 2 Cytotoxic activities of GLA and its partially deuterated derivatives **7a–7c** towards VA-13 and WI-38 cells.

VA-13 cells than WI-38 cells, confirming the reported tumor-selective cytotoxicity, although the difference between the effective doses for the two cell lines was not large. Next, the effects of metabolism on the cytotoxicity were examined by using deuterated GLA derivatives **7a–7c**. Interestingly, none of these partially deuterated GLA was cytotoxic to WI-38 cells even at 200 μM, indicating that the cytotoxicity of GLA to normal cells depends on metabolic and/or chemical reaction at the bis-allylic positions. To support this speculation, we also compared the reactivities between GLA and deuterated GLA to the enzymatic oxidation, which confirmed the metabolic inhibition of GLA by the deuteration of bis-allylic methylenes (Fig. S1, ESI†). In contrast, deuteration at the C8 and/or C11 positions only slightly decreased the cytotoxicity of GLA to VA-13 cells. These results indicate that different cell-death-inducing mechanisms are operative in normal and tumor cells. In the case of VA-13 tumor cells, reaction at the bis-allylic position is not critical. GLA itself or its metabolites generated by reaction at some other position(s) might be involved in the cytotoxicity towards tumor cells. To clarify this point, we next synthesized fully deuterated GLA (all-D-GLA). If abstraction of any of the hydrogen atoms in GLA is critical for the production of the key metabolite(s), the cytotoxicity of all-D-GLA should be further decreased.

As shown in Scheme 2, deuterated methyl 6-heptynoate **9** was prepared from deuterated cyclohexene **8**.<sup>23,24</sup> The fully



**Scheme 1** Synthesis of partially deuterated GLA derivatives. *Reagents and conditions:* (a) (i) *n*BuLi, (CD<sub>2</sub>O)<sub>*n*</sub>, THF, 0 °C; (ii) DHP, *p*-TsOH·H<sub>2</sub>O, DCM, (iii) TBAF, THF, 0 °C; (b) (i) *n*BuLi, (CX<sub>2</sub>O)<sub>*n*</sub>, THF, (ii) TsCl, K<sub>2</sub>CO<sub>3</sub>, 1-hexadecylimidazole, H<sub>2</sub>O; (c) (i) propargyl alcohol, CuI, K<sub>2</sub>CO<sub>3</sub>, NaI, DMF, (ii) TsCl, K<sub>2</sub>CO<sub>3</sub>, 1-hexadecylimidazole, H<sub>2</sub>O; (d) (i) **2**, CuI, K<sub>2</sub>CO<sub>3</sub>, NaI, DMF, (ii) *p*-TsOH·H<sub>2</sub>O, MeOH, (iii) TsCl, K<sub>2</sub>CO<sub>3</sub>, 1-hexadecylimidazole, H<sub>2</sub>O; (e) (i) methyl 6-heptynoate, CuI, K<sub>2</sub>CO<sub>3</sub>, NaI, DMF, (ii) H<sub>2</sub>, NaBH<sub>4</sub>, Ni(OAc)<sub>2</sub>, ethylenediamine, MeOH; (f) LiOH·H<sub>2</sub>O, THF, H<sub>2</sub>O.



**Scheme 2** Synthesis of fully deuterated GLA. *Reagents and conditions:* (a) (i) O<sub>3</sub>, NaHCO<sub>3</sub>, DCM, CD<sub>3</sub>OD, –78 °C; (ii) Ac<sub>2</sub>O, NEt<sub>3</sub>, DCM, (iii) Ohira–Bestmann reagent, K<sub>2</sub>CO<sub>3</sub>, CD<sub>3</sub>OD, 0 °C; (b) (i) *n*BuLi, C<sub>5</sub>D<sub>11</sub>Br, HMPA, THF, (ii) *p*-TsOH·H<sub>2</sub>O, MeOH, (iii) TsCl, K<sub>2</sub>CO<sub>3</sub>, 1-hexadecylimidazole, H<sub>2</sub>O; (c) (i) **2**, CuI, K<sub>2</sub>CO<sub>3</sub>, NaI, DMF, (ii) *p*-TsOH·H<sub>2</sub>O, MeOH, (iii) TsCl, K<sub>2</sub>CO<sub>3</sub>, 1-hexadecylimidazole, H<sub>2</sub>O; (d) (i) **9**, CuI, K<sub>2</sub>CO<sub>3</sub>, NaI, DMF, (ii) D<sub>2</sub>, NaBD<sub>4</sub>, Ni(OAc)<sub>2</sub>, ethylenediamine, CD<sub>3</sub>OD; (e) LiOH·H<sub>2</sub>O, THF, H<sub>2</sub>O.

deuterated C8–C18 unit **11** was synthesized from **10**, which was prepared from deuterated pentyl bromide and **2**. Then **11** was converted to **12** by coupling reaction with **9** and partial reduction using  $D_2$ . Finally, all-D-GLA was obtained by hydrolysis of the ester moiety.

All-D-GLA was tested for cytotoxicity towards WI-38 and VA-13 cells (Fig. 3). It proved to be cytotoxic to VA-13 cells, but not WI-38 cells, like the partially deuterated derivatives **7a–7c**. This result suggests that GLA itself, but not its metabolites, is cytotoxic to tumor cells.

The non-specific cytotoxicity of GLA may be due to the products of enzymatic oxidation or non-specific peroxidation of GLA, and suppression of these reactions by deuteration may account for the increased tumor-selectivity. Thus, all-D-GLA may be preferable to GLA for analyzing the mechanism of the tumor-selectivity.

In addition to the improved activity, all-D-GLA is expected to show a sufficiently strong Raman signal for live-cell imaging, which would be useful to gain mechanistic insights into the tumor-selective cytotoxicity of GLA. To confirm the Raman signals resulting from deuteration, Raman spectra of GLA and deuterated GLAs were obtained by means of Raman microscopy (Fig. 4 and Fig. S2, ESI†). As shown in Fig. 4, all-D-GLA showed strong Raman signals due to C–D bonds ( $2000–2300\text{ cm}^{-1}$ ) in the cellular silent region. In contrast, the strong Raman signals corresponding to C–H bonds ( $2800–3100\text{ cm}^{-1}$ ) seen in the spectrum of GLA were completely absent in the spectrum of all-D-GLA. These observations confirmed the successful complete deuteration of GLA. Moreover, deuteration shifted the Raman signal of the carbon–carbon double bond (C=C) from  $1660\text{ cm}^{-1}$  (GLA) to  $1630\text{ cm}^{-1}$  (deuterated GLA), in good agreement with a previous report.<sup>17,25</sup> Therefore, we also examined whether the Raman signal of the DC=CD bond could be used as a Raman tag for live-cell imaging, in addition to the C–D bond signal.

VA-13 cells were treated with all-D-GLA ( $100\text{ }\mu\text{M}$ ) and observed by Raman microscopy at each indicated time (Fig. 5 and Fig. S3, ESI†). Raman images were constructed from the Raman peaks at  $1630$ ,  $2115$ ,  $2854$ ,  $3015\text{ cm}^{-1}$ . The cellular distribution of all-D-GLA was successfully visualized by using the Raman signal at  $2115\text{ cm}^{-1}$ , corresponding to the D–C–D bond. Time-dependent accumulation of GLA in the cells was observed. Interestingly, essentially identical images were

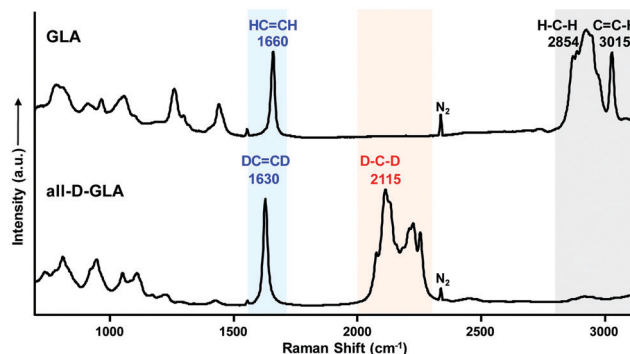


Fig. 4 Raman spectra of GLA and all-D-GLA.

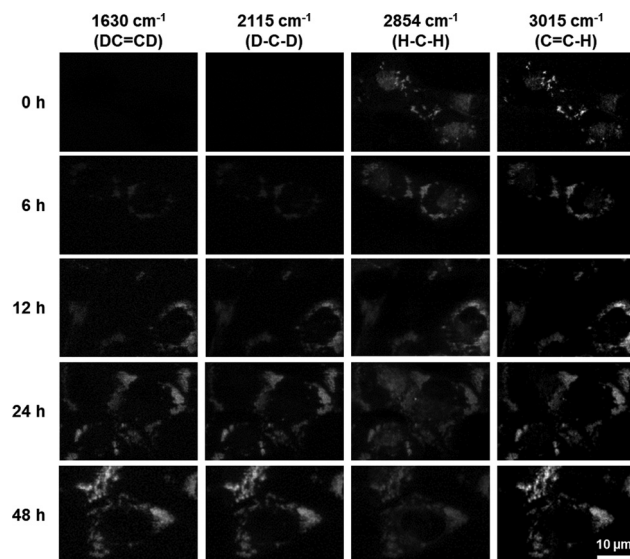


Fig. 5 Raman images of VA-13 cells treated with  $100\text{ }\mu\text{M}$  all-D-GLA.

obtained by using the signal of DC=CD at  $1630\text{ cm}^{-1}$ , indicating the potential of the DC=CD bond as a Raman tag for live-cell imaging.

Compared with the cellular distributions of the H–C–H signal at  $2854\text{ cm}^{-1}$  and the C=C–H signal at  $3015\text{ cm}^{-1}$ , all-D-GLA showed good colocalization with the C=C–H distribution, which was reported to be a marker of lipid droplets (LDs) corresponding to triglyceride.<sup>26</sup> Therefore, all-D-GLA is thought to accumulate in LDs to exert its cytotoxicity. Although the precise mechanism is still unclear, several reports indicate that the formation of LDs is important for the proliferation of cancer cells.<sup>27,28</sup> LDs store fatty acids as triglyceride or cholesteryl ester, and cancer cells use LD-derived fatty acids as an energy source for proliferation through mitochondrial  $\beta$ -oxidation. All-D-GLA remained in LDs, and was not incorporated into mitochondria (Fig. S3, ESI†), suggesting that it might inhibit cancer cell proliferation, leading to induction of cell death.

Next, Raman imaging of WI-38 cells was examined (Fig. 6 and Fig. S4, ESI†). WI-38 cells were treated with all-D-GLA

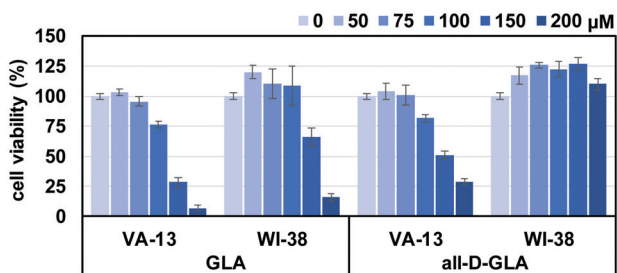


Fig. 3 Cytotoxic activities of GLA and all-D-GLA towards VA-13 and WI-38 cells.

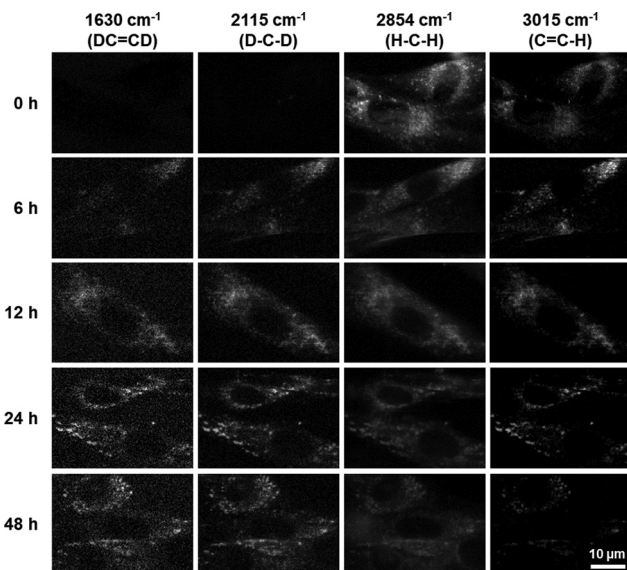


Fig. 6 Raman images of WI-38 cells treated with 100  $\mu\text{M}$  all-D-GLA.

(100  $\mu\text{M}$ ), and Raman images were taken in the same manner as described for VA-13 cells. Initially, all-D-GLA was accumulated into LDs, as in VA-13 cells, but as the incubation time increased, the Raman signal of C–D bond was also observed outside of LDs. It is noteworthy that the H–C–H and C=C–H signals decreased gradually as all-D-GLA was incorporated (Fig. 6, Fig. S5A and S6, ESI<sup>†</sup>). These changes imply the metabolic replacement of cellular fatty acids by all-D-GLA. In addition to serving as an energy source in mitochondria, fatty acids are also used to synthesize membrane phospholipids. This step would not require modification of the deuterated methylenes. Therefore, excess all-D-GLA in LDs might be used for membrane synthesis in WI-38 cells. We also constructed merged images from the D–C–D signal and C=C–H signal (Fig. S5B, ESI<sup>†</sup>), and these clearly visualized the difference of cellular distribution of all-D-GLA between VA-13 and WI-38 cells. In VA-13 cells, all-D-GLA stayed in LDs. In contrast, in WI-38 cells, all-D-GLA distributed throughout the cell, though it partly colocalized with LDs. This observation implies that WI-38 cells could use GLA in the same manner as other PUFAs. In Fig. 2 and 3, deuterated GLA improved the cell viability of WI-38 cells up to 125% compared with control cells. Recent study reported the improvement of cell viability of embryonic cells by the treatment with  $\alpha$ -linolenic acid (ALA).<sup>29</sup> Although the detailed mechanism is unclear, GLA might have the same activity to WI-38 cells.

In conclusion, we have synthesized partially/fully deuterated GLA, and established an assay system using VA-13/WI-38 cells to examine the reported tumor-selective cytotoxicity of GLA. Deuteration of GLA increased the selectivity for tumor cells, suggesting that GLA itself, but not its oxidized metabolites, mediates the tumor-selective cytotoxicity. Raman imaging of all-D-GLA revealed its accumulation in LDs. A difference of LD-related metabolism between tumor and normal cells might be responsible for the tumor-selective cytotoxicity of GLA. Further mechanistic studies are in progress.

This work was supported by AMED-CREST, AMED under Grant Number JP18gm071004 (M. S.). This work was also supported by JST CREST Grant Number JPMJCR1925 (M. S.), MEXT KAKENHI Grant Number JP26110004 (M. S. and K. D.), and JSPS KAKENHI Grant Number JP18K14360 and JP20K15418 (S. E.). S. E. was supported by the Special Postdoctoral Researchers' Program in RIKEN.

## Conflicts of interest

There are no conflicts to declare.

## Notes and references

- C. D. Funk, *Science*, 2001, **294**, 1871–1875.
- M. J. Mueller, *Chem. Biol.*, 1998, **5**, R323–R333.
- I. de Bus, R. Witkamp, H. Zuillhof, B. Albada and M. Balvers, *Prostaglandins Other Lipid Mediators*, 2019, **144**, 106351.
- U. N. Das, *Med. Sci. Monit.*, 2007, **13**, RA119–RA131.
- U. N. Das, *Cancer Lett.*, 1991, **56**, 235–243.
- P. Sangeetha Sagar, U. N. Das, R. Koratkar, G. Ramesh, M. Padma and G. Sravan Kumar, *Cancer Lett.*, 1992, **63**, 189–198.
- Q. Yu, Z. Shan, K. Ni and S. Y. Qian, *Free Radical Res.*, 2008, **42**, 442–455.
- M. A. Fomich, A. V. Bekish, D. Vidovic, C. R. Lamberson, I. L. Lysenko, P. Lawrence, J. T. Brenna, O. L. Sharko, V. V. Shmanai and M. S. Shchepinov, *ChemistrySelect*, 2016, **1**, 4758–4764.
- A. R. Navratil, M. S. Shchepinov and E. A. Dennis, *J. Am. Chem. Soc.*, 2018, **140**, 235–243.
- S. Hill, C. R. Lamberson, L. Xu, R. To, H. S. Tsui, V. V. Shmanai, A. V. Bekish, A. M. Awad, B. N. Marbois, C. R. Cantor, N. A. Porter, C. F. Clarke and M. S. Shchepinov, *Free Radical Biol. Med.*, 2012, **53**, 893–906.
- A. M. Firsov, M. A. Fomich, A. V. Bekish, O. L. Sharko, E. A. Kotova, H. J. Saal, D. Vidovic, V. V. Shmanai, D. A. Pratt, Y. N. Antonenko and M. S. Shchepinov, *FEBS J.*, 2019, **286**, 2099–2117.
- H. J. Van Manen, A. Lenferink and C. Otto, *Anal. Chem.*, 2008, **80**, 9576–9582.
- H. Yamakoshi, K. Dodo, A. Palonpon, J. Ando, K. Fujita, S. Kawata and M. Sodeoka, *J. Am. Chem. Soc.*, 2012, **134**, 20681–20689.
- H. Yamakoshi, K. Dodo, M. Okada, J. Ando, A. Palonpon, K. Fujita, S. Kawata and M. Sodeoka, *J. Am. Chem. Soc.*, 2011, **133**, 6102–6105.
- A. F. Palonpon, J. Ando, H. Yamakoshi, K. Dodo, M. Sodeoka, S. Kawata and K. Fujita, *Nat. Protoc.*, 2013, **8**, 677–692.
- L. Wei, F. Hu, Y. Shen, Z. Chen, Y. Yu, C. C. Lin, M. C. Wang and W. Min, *Nat. Methods*, 2014, **11**, 410–412.
- H.-J. van Manen, Y. M. Kraan, D. Roos and C. Otto, *Proc. Natl. Acad. Sci. U. S. A.*, 2005, **102**, 10159–10164.
- X. S. Xie, J. Yu and W. Y. Yang, *Science*, 2006, **312**, 228–230.
- K. Asano and S. Matsubara, *Org. Lett.*, 2009, **11**, 1757–1759.
- M. P. Meyer and J. P. Klinman, *Tetrahedron Lett.*, 2008, **49**, 3600–3603.
- P. Bhar, D. W. Reed, P. S. Covello and P. H. Buist, *Angew. Chem., Int. Ed.*, 2012, **51**, 6686–6690.
- T. Jeffery, S. Gueugnot and G. Linstrumelle, *Tetrahedron Lett.*, 1992, **33**, 5757–5760.
- R. E. Claus and S. L. Schreiber, *Org. Synth.*, 1986, **64**, 150.
- J. Pietruszka and A. Witt, *Synthesis*, 2006, 4266–4268.
- H. W. Schrötter and E. G. Hoffmann, *Justus Liebigs Ann. Chem.*, 1964, **672**, 44–54.
- D. Fu, Y. Yu, A. Follick, E. Currie, R. V. Farese, T.-H. Tsai, X. S. Xie and M. C. Wang, *J. Am. Chem. Soc.*, 2014, **136**, 8820–8828.
- S. Koizume and Y. Miyagi, *Int. J. Mol. Sci.*, 2016, **17**, 1430.
- Q. Liu, Q. Luo, A. Halim and G. Song, *Cancer Lett.*, 2017, **401**, 39–45.
- R. Mahmoudi, M. Ghareghani, K. Zibara, M. Tajali Ardakani, Y. Jand, H. Azari, J. Nikbakht and A. Ghanbari, *BMC Complementary Altern. Med.*, 2019, **19**, 113.